










## Article

# Bio-Compatibility Analysis of Newly Developed Plug and Cuff Electrodes for Future Neuronal Interface Applications

Eleni Zingkou<sup>1,\*</sup>, Georgios Pampalakis<sup>1,\*</sup>, Asimina Kolianou<sup>1</sup>, Nafsika Rossopoulou<sup>2</sup>, Aikaterini Skiada<sup>2</sup>, Lydia Galouni<sup>2</sup>, Patryk Śniarowski<sup>3,4</sup>, Longina Madej-Kiełbik<sup>3</sup>, Georgia Sotiropoulou<sup>1</sup>, Karolina Gzyra-Jagiela<sup>3</sup>, Theodora Katsila<sup>2</sup>, Carmen Moldovan<sup>5</sup>, Marian Ion<sup>5</sup>, Octavian Narcis Ionescu<sup>5</sup>, Eduard Franti<sup>5</sup>, David Dragomir<sup>5</sup>, Gerd Siekmeyer<sup>6</sup> and Patrick Grotemeyer<sup>6</sup>

<sup>1</sup> Department of Pharmacy, School of Health Sciences, University of Patras, 26504 Rion-Patras, Greece; asiminakolianou@ac.upatras.gr (A.K.); gdsotiro@upatras.gr (G.S.)

<sup>2</sup> Institute of Chemical Biology, National Hellenic Research Foundation, 48 Vasileos Constantinou Avenue, 11635 Athens, Greece; rossopn@eie.gr (N.R.); kskiada@eie.gr (A.S.); lgalouni@eie.gr (L.G.); thkatsila@eie.gr (T.K.)

<sup>3</sup> Łukasiewicz Research Network, Łódź Institute of Technology, Marii Skłodowskiej-Curie 19/27 St, 90-570 Łódź, Poland; patryk.sniarowski@lit.lukasiewicz.gov.pl (P.Ś.);

longina.madej-kiełbik@lit.lukasiewicz.gov.pl (L.M.-K.); karolina.gzyra-jagiela@lit.lukasiewicz.gov.pl (K.G.-J.)

<sup>4</sup> Interdisciplinary Doctoral School, Łódź University of Technology, Żeromskiego 116 St, 90-924 Łódź, Poland

<sup>5</sup> IMT Bucharest, 77190 Bucharest, Romania; carmen.moldovan@imt.ro (C.M.); marian.ion@imt.ro (M.I.);

octavian.ionescu@imt.ro (O.N.I.); eduard.franti@imt.ro (E.F.); david.dragomir@imt.ro (D.D.)

<sup>6</sup> Acquandas-Kaiserstraße 2, Building F, 1st floor room F-021, 24143 Kiel, Germany;

siekmeyer@acquandas.com (G.S.); grotemeyer@acquandas.com (P.G.)

\* Correspondence: zingkou@upatras.gr (E.Z.); gpampalakis@pharm.auth.gr (G.P.); Tel.: +30-2610-962-316 (E.Z.)

† Current address: School of Pharmacy, Aristotle University of Thessaloniki, 54124 Thessaloniki, Greece.

## Abstract

The NerveRepack project is a European initiative that aims to develop biomimetic exoskeletons/exoprostheses for amputated or paralyzed leg patients that will receive and transmit signals to enable movements and sensations for the patient. To implement the project, it is fundamental to develop implantable neuronal electrodes that will allow bidirectional signaling between the sensors placed on the exoskeletons/exoprostheses and the nervous system. In this direction, two electrodes, plug and cuff, have been designed as integral parts of the final implantable device. The electrodes should comply with strict regulations to ensure their safe implantation in patients. The purpose of this study was to support the compliance of the implant platforms of certain key components with the ISO and ASTM standards that would be required for clinical applications. We have used an indirect method to assess the biocompatibility of the developed electrodes against neuronal cells, fibroblasts, and keratinocytes. Also, we assessed hemocompatibility, i.e., the potential of implantable electrodes to induce hemolysis or complement activation. Finally, the mutagenic/genotoxic potential was tested against the internationally recommended CHO cells. Both representative plug and cuff electrode components were found non-cytotoxic, non-mutagenic, and unable to induce hemolysis. Therefore, from the point of early evaluation of in vitro material and process biocompatibility, the selected implant platforms for the electrodes could be implanted in preclinical models to delineate their potential in vivo applications as neuronal interface with the biomimetic exoskeleton/exoprostheses.

**Keywords:** cuff electrode; plug electrode; neuronal interface; biocompatibility



Academic Editors: Hyeonseok Kim, Jihwan Lee and Abdulhameed Abdal

Received: 21 November 2025

Revised: 9 January 2026

Accepted: 15 January 2026

Published: 16 February 2026

**Copyright:** © 2026 by the authors.

Licensee MDPI, Basel, Switzerland.

This article is an open access article

distributed under the terms and

conditions of the [Creative Commons](https://creativecommons.org/licenses/by/4.0/)

[Attribution \(CC BY\)](https://creativecommons.org/licenses/by/4.0/) license.

## 1. Introduction

In recent years, there has been a dynamic development of neural interface technologies aimed to enable direct communication between the nervous system and electronic devices. The scientific literature highlights the importance of biocompatible and flexible electrodes, particularly the cuff and plug types, which allow for long-term, stable, and selective interaction with peripheral nerves. Research in this field focuses on selecting appropriate materials and structures that minimize immune responses, while improving the durability and functionality of interfaces under biological conditions, representing a crucial step toward the advancement of sophisticated neuroprosthetic systems and regenerative therapies [1–6]. Currently, scientific research focuses on advances in neural interface engineering, with particular emphasis on the development of new materials, including flexible, biocompatible, and minimally invasive electrodes that improve the stability and efficiency of neural connections. Great importance is also placed on modern fabrication techniques and the use of nanostructures to enhance signal quality and promote long-term integration of electrodes with neural tissue [7]. Ranke et al. also emphasize the importance of selecting appropriate materials for electrodes used in neural interfaces, as they determine biocompatibility, conductivity, and durability in biological environments [8].

Neural electrodes are essential components of neuroprosthetic devices, enabling the bidirectional communication between the nervous system and external hardware. Existing devices, including penetrating microelectrodes (e.g., Utah array, Michigan probes) and peripheral nerve sleeves (e.g., silicone-based sleeves), have advanced the field, but face persistent limitations associated with mechanical mismatch, biocompatibility, and long-term stability (Table 1) [9].

**Table 1.** Existing neural electrodes: overview and limitations.

Electrode Type	Materials	Geometries	Mechanical Objectives	Limitations
Utah Array	Silicon, Platinum, Iridium Oxide (IrOx)	Microelectrodes (~60 $\mu\text{m}$ diameter, 1–2 mm length)	High spatial resolution, penetrating	Biocompatibility issues, tissue response, limited longevity
Michigan Probes	Silicon Shanks (~10–50 $\mu\text{m}$ width)	Penetrating shanks	Precise, high-density recordings	Brittle, poor mechanical compliance, tissue damage risk
Nerve Cuff Electrodes	Silicone and Platinum (rarely coated with IrOx)	Spiral or cylindrical cuffs (~3–6 mm diameter)	Conform around nerves, flexible	Encapsulation fibrosis, limited selectivity, low charge injection and charge storage capacity, invasive deployment

Pre-existing neural interface devices face significant limitations related to their mechanical properties. Rigid, silicon-based electrodes often exhibit mechanical incompatibility with soft neural tissue, which can trigger inflammatory reactions and lead to fibrotic encapsulation, ultimately impairing interactions between electrodes and nerves [9].

In addition, many conventional designs suffer from limited long-term stability. Material degradation and sustained immune reactions can progressively compromise signal quality, reducing the reliability of neural recordings over time [10]. The invasive nature of penetrating devices further increases the risk of nerve damage, making their long-term and chronic application difficult. For the NerveRepack implementation, we propose the use of materials outlined in Table 2 for the construction of plug and cuff electrodes.

**Table 2.** Design Rationale: Material Choices.

Material	Rationale	Properties and Benefits
Nitinol (Nickel-Titanium)	Super elasticity, shape-memory	Reduces mechanical mismatch, accommodates nerve movements, minimizes tissue trauma [11]
Polyurethane (TPU)	Soft, flexible encapsulation	Biocompatibility, elasticity matching nerve tissue, reduces foreign body response [12]
Gold Films (~10–15 $\mu\text{m}$ thick)	Conductive, inert, superior carrier substrate for future coatings (improve electric characteristics)	Stable electrical contacts, corrosion resistance, minimal tissue reactivity [13]
Stainless Steel Needles	Structural rigidity	Precise, durable insertion points

Biocompatibility ensures the safe implantation of the biomedical device, including electrodes, in the body without causing any harm or adverse reactions. Therefore, very strict regulations and standards have been established to protect human health and life, making biocompatibility assessment an essential component of research and development in neural interface technologies. Likewise, in the European Union, medical devices are subject to very strict legal regulations and standards. The current legal framework is established by Regulation (EU) 2017/745 on medical devices, which requires the assessment of the safety and performance of devices before they are placed on the market. An important part of this assessment involves biological evaluation in accordance with the International Organization for Standardization (ISO) 10993 [14–17] and the American Society for Testing and Materials (ASTM) standards [18–21]. These include, among others, tests for cytotoxicity, genotoxicity, hemocompatibility, and the long-term biocompatibility of materials. The application of these standards ensures a comprehensive verification of whether the materials used in medical devices are safe for the human body and suitable for their intended clinical use [22–24].

In the present study, we have evaluated the biocompatibility of new electrodes for neural implantation and neural interface applications. The findings represent an initial *in vitro* safety screen and are a prerequisite for further steps (*in vivo* biocompatibility, fibrosis assessment, nerve conduction/stimulation validation). These electrodes were designed to transmit neuronal signals acting as command signals for exoprostheses or exoskeletons translated into movements, and to receive signals from the sensors placed on exoprostheses and exoskeletons to be translated into sensations for the user. These electrodes are referred to as plug and cuff electrodes. Their detailed structure and construction will be the subject of a future paper, and here we focus only on the biocompatibility aspects of key representative components from materials and processes. Briefly, the plug electrode is composed of three needles with a sharp tip and a rod with a length of 15 mm with a diameter of 100  $\mu\text{m}$ . Each needle is made of stainless steel covered with a 200 nm conducting layer of gold with a 15 nm titanium layer in the middle to assist in gold adherence. The needles are encapsulated in a 3D printed holder composed of gelatin methacryloyl. The plug electrode achieves bidirectional connections of exoprostheses with the peripheral nervous system of patients with upper limb amputation (Figure 1A). Specifically, the plug electrodes have been designed to be implanted in the cross-section of the median and ulnar nerve. The median nerve encompasses the motor and sensory fascicles for the thumb, index, and middle finger, while the ulnar nerve for the ring and little finger, respectively. The bidirectional connection creates a closed loop between the users' brains and the control block of the exoprosthesis.

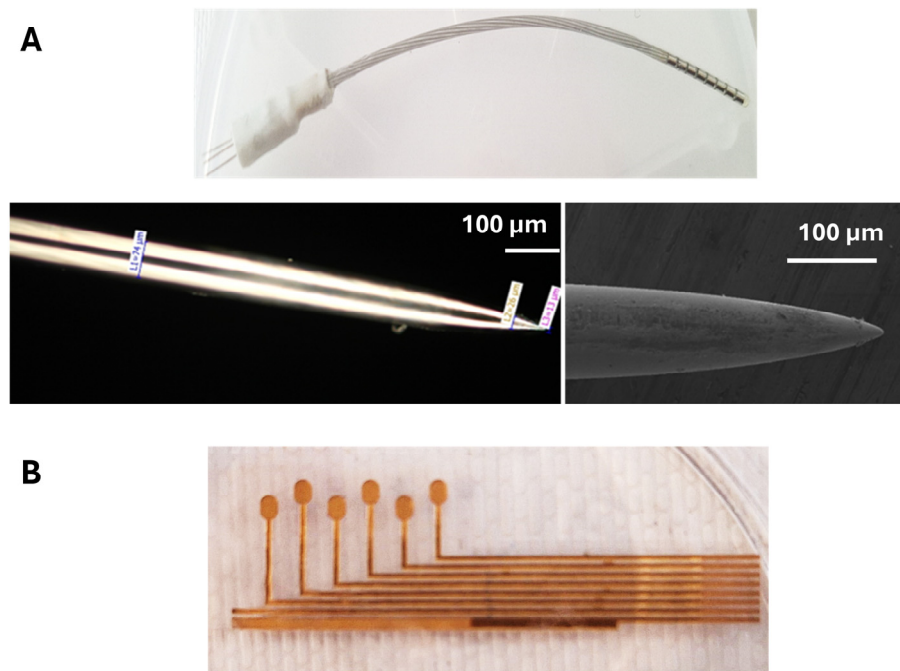


**Figure 1.** Structure of the plug and the cuff electrodes. **(A).** Structure of the plug electrodes. **(Upper)** Macroscopic appearance of the plug electrode where the three gold-covered needles are shown on the left. **(Lower)** SEM picture of gold covered needle. **(B).** Macroscopic structure of the thermoplastic polyurethane (TPU) bearing gold electrode stack part of the cuff electrode.

The development and validation of plug electrodes began with a careful process of design and material selection. Gold-coated stainless-steel needles were chosen as the main conductive elements, incorporating a titanium adhesion layer to ensure a robust bond between the substrate and the gold coating. This combination was selected to balance electrical performance, mechanical stability, and biocompatibility.

Fabrication involved the use of 3D printing to produce a customized support that allows for precise alignment and secure positioning of the needles. The electrodes were then assembled by integrating the gold-coated needles into the printed support, resulting in a reproducible and scalable plug-type electrode configuration. An *in vitro* biological assessment was conducted to evaluate the safety profile of the electrodes. Cytotoxicity was examined using multiple cell lines, including SH-SY5Y neuroblastoma cells, fibroblasts, and keratinocytes to capture responses relevant to neuronal and surrounding tissues. Additional assessment included hemocompatibility and mutagenicity tests to evaluate potential adverse interactions with blood components and genetic material.

Cuff electrodes are extraneuronal electrodes used to wrap the neuron. Traditional cuff electrodes are silicone-based and rigid, although recent attempts have been made to generate soft cuff electrodes [25]. The advantage of soft and stretchable cuff electrodes is their ability to allow for selective stimulation of portions of the nerve which is important for therapeutic applications. Also, mechanical softness is associated with reduced foreign body response. In this direction, cuff electrodes used here are built from a stack made of nitinol mesh, of 35 μm thickness, embedded in 10 μm thermoplastic polyurethane (TPU), a TPU foil carrier with thickness of 50 μm and gold tracks of 10 μm thickness embedded in 10 μm TPU. The TPU membrane on the nerve and connector side has been stripped for electric contact. The nerve cuff electrode has eight gold channels with a pitch of 0.5 mm and a conductor width of 0.3 mm (Figure 1B).

The flexible cuff electrode and the plug electrodes presented in this study represent a step toward more biocompatible and mechanically compliant neural interfaces. By

integrating advanced materials and optimized geometries, these designs address several limitations associated with earlier rigid and invasive electrodes, supporting improved stability for stable long-term neuroprosthetic applications.

## 2. Materials and Methods

### 2.1. Materials

All chemicals used were obtained from Merck (Darmstadt, Germany). All culture media were obtained from Gibco (Thermo Fisher Scientific, Waltham, MA, USA) unless otherwise stated. Human blood and sheep red blood cells (RBCs) were obtained from Dunn Labortechnik GmbH (Asbach, Germany).

### 2.2. SH-SY5Y and Differentiation

The SH-SY5Y cells were kindly provided by Kostas Vekrellis (Biomedical Research Foundation of the Academy of Athens, Athens, Greece) and were cultured in DMEM medium containing pyruvate supplemented with 10% fetal bovine serum (FBS) and 1% penicillin/streptomycin at 37 °C in a humidified incubator with an atmosphere of 5% CO<sub>2</sub>. For subculturing, when SH-SY5Y reached ~70–80% confluency, the medium was discarded and trypsin/EDTA solution was added, followed by incubation at 37 °C until cell detachment. Then, the trypsin was inhibited by adding two volumes of phosphate-buffered saline (PBS) containing 10% FBS. The cell suspension was collected and centrifuged at 1000× *g* for 5 min, followed by resuspension of the cell pellet in fresh medium and transfer to new culture flasks. Microscopic evaluation of the cells in culture was performed with an inverted optical microscope (Carl Zeiss, Jena, Germany). For the differentiation of SH-SY5Y cells to neuronal-like cells, SH-SY5Y were plated on plastic dishes and after 24 h incubated with 10 μM retinoic acid (RA) for 7 days.

### 2.3. Fibroblasts

Normal dermal human fibroblasts (NDHFs) were kindly provided by Dr. Dimitra Kiritsi (Department of Dermatology, University of Freiburg, Freiburg, Germany) cultured in DMEM medium supplemented with 10% FBS, 2% L-glutamine, and 1% penicillin/streptomycin at 37 °C in a humidified incubator with an atmosphere of 5% CO<sub>2</sub>. Subculturing was carried out as described for SH-SY5Y.

### 2.4. Chinese Hamster Ovary Cells

CHO cells were kindly provided by Kostas Vekrellis (Biomedical Research Foundation of the Academy of Athens, Athens, Greece) and were cultured in a humidified incubator at 37 °C in 5% CO<sub>2</sub> and maintained as adherent culture in F-12K medium (Kaighn's Modification of Ham's F-12 Medium) (Biowest, Nuaille, France) supplemented with 1% penicillin/streptomycin and 10% FBS (Corning, Glendale, AZ, USA). Subculturing was carried out as described above. In greater detail, CHO cells were detached from the surface during subculturing by the use of a pre-warmed trypsin/disodium ethylene diamine tetra acetic acid (EDTA) solution (Gibco, Thermo Fisher Scientific, Waltham, MA, USA), followed by incubation for 5 min at 37 °C. Trypsin was inactivated by the addition of three volumes of complete culture medium. Cell suspension was collected and centrifuged at 1000 rpm for 5 min. After centrifugation supernatant was discarded and the pellet was resuspended in fresh complete medium. The appropriate number of cells was transferred to a new culture flask for cell growth. Cell viability was assessed by using a glass hemocytometer and trypan blue exclusion test. Cell counting and concentration (viable cells/mL) were calculated automatically via the automated Axion Biosystems platform. No experiment was performed unless cell viability was higher than 95%.

### 2.5. HaCaT Cells

HaCaT cells were obtained from Cytion GmbH (Heidelberg, Germany). HaCaT is a spontaneously immortalized human keratinocyte cell line. It was cultured in DMEM supplemented with 10% FBS, and 1% Antibiotic-Antimycotic solution (Sigma-Aldrich, St. Louis, MO, USA) at 37 °C in a humidified incubator in an atmosphere of 5% CO<sub>2</sub>. Subculturing was carried out as described.

### 2.6. Preparation of Extracts

For evaluating the compatibility of the provided materials, a sterilization procedure prior to experiments involving cells was performed. Materials were sterilized by exposure to UV for 10 min per side inside a biosafety class II cabinet. The time of sterilization was agreed among the partners of the program and is also based on previous studies [26]. Gentle handling and strict aseptic techniques were essential to ensure cell viability and prevent contamination. The extracts were prepared according to part 12, "Sample preparation and reference materials" of ISO 10993 [17]. Specifically, the plug and cuff electrodes were incubated in serum-free culture medium for 72 h at 37 °C. The extracts were collected, and supplemented with serum (10%), in order to be administered to cells. The electrode to culture medium ratios were decided according to the corresponding ISO guidelines based on the mass for plug electrode, and on the surface area for cuff electrode.

### 2.7. Exposure of Cells to the Extract (Indirect Cytotoxicity)

Following viability testing, the cell suspension was adjusted to a final density of  $1 \times 10^6$  cells/mL. Subsequently, 100 µL of the suspension was seeded into the wells of a sterile 96-well plate. Such cell density ensured even coverage of the well surface. The cells were incubated for 24 h at 37 °C with 5% CO<sub>2</sub> to allow the formation of a uniform monolayer. Subsequently, the cells were exposed to the extract described above.

### 2.8. Cytotoxicity Assessment Based on MTT

3-(4,5-dimethylthiazol-2-yl)-2,5-diphenyltetrazolium bromide or MTT is a water-soluble yellow tetrazolium dye which can be reduced to insoluble blue formazan by oxidoreductases in the mitochondria of viable cells. The intensity of the yielded color is correlated to the number of viable cells. A solution of MTT in sterile PBS was prepared fresh (5 mg/mL), mixed by vortexing, and filter sterilized. The MTT solution was then combined with an equal volume of DMEM without serum and applied to the cells (100 µL per well). The cells were incubated at 37 °C for approximately 3 h or until blue formazan crystals were visible when examining the cells under the microscope. The MTT medium was removed and 100 µL dimethyl sulfoxide were added in each well to dissolve the formazan crystals. The absorbance was measured in a plate reader at 570 nm. For each experiment, blanks, untreated cells, and cells treated with 1% SDS were included as controls.

### 2.9. Cytotoxicity Assessment Based on Neutral Red Uptake (NRU)

When the cells were exposed to the tested extract for 24 h, a stock solution of NR in sterile water (0.4%) was prepared and filter sterilized. One day prior to testing, NR solution was added to culture medium (1:80) and incubated at 37 °C overnight. The following day, the NR medium was filtered to discard NR crystals that may have formed. Culture medium was then removed, the cells were washed with PBS and the NR medium was added to each well, including the blanks (100 µL per well). The plates were incubated at 37 °C for 1–3 h and then the NR medium was discarded. The cells were washed with PBS (150 µL) and a destaining solution was added to the wells (50% ethanol, 1% acetic acid). The absorbance was recorded with a plate reader at 540 nm.

### 2.10. Cytotoxicity Assessment Based on Alamar Blue

This method was incorporated into the extract test while assessing the genotoxicity and/or carcinogenicity of the materials tested. In detail, Alamar Blue assay is a reliable method used to evaluate cellular metabolic activity, serving as an indirect measure of cell viability. The assay relies on the reduction of non-fluorescent resazurin to the fluorescent, resorufin by metabolically active cells [27]. To perform the assay, once the cells (control and test conditions of the genotoxicity assay) were ready for analysis, a working solution of Alamar Blue (Invitrogen, Thermo Fisher Scientific, Waltham, MA, USA) reagent was prepared (10% *v/v* in the culture medium) and added to the wells, where the same amount of culture medium was removed, ensuring even coverage in all wells. Cells were incubated at 37 °C with 5% CO<sub>2</sub> for 4 h. After incubation, absorbance measurements were carried out at an excitation wavelength of 570 nm and an emission wavelength of 600 nm. For normalization and accuracy, wells with culture medium and Alamar Blue solution without cells as a blank control were also included. The absorbance intensity correlates directly with cell metabolic activity, allowing for quantification and comparison between experimental conditions.

### 2.11. In Vitro Mammalian Cell Micronucleus Assay

The genotoxic and/or carcinogenicity potential of the tested materials was assessed using the in vitro mammalian cell micronucleus assay, following established protocols. This assay is a standardized method used to evaluate genotoxicity and/or carcinogenicity by detecting the formation of micronuclei in the cytoplasm of interphase cells, indicative of chromosomal damage or missegregation. The assay can be performed in vitro on cultured mammalian cells or in vivo on bone marrow or peripheral blood erythrocytes, in compliance with ISO 10993-3 [15], OECD guidelines, and ECVAM recommendations. For in vitro testing, CHO cells (50,000 cells/mL) were seeded in 8-well chamber  $\mu$ -slide (ibiTreated) (Ibidi GmbH, Gräfelfing, Germany) and then incubated at 37 °C, 5% CO<sub>2</sub> for 18 h, allowing them to grow to 60–80% confluency. Cells were treated with the extracts from the materials, including a negative control (vehicle only) and positive controls for 6 h to imitate short exposure and 24 h for extended exposure of the cells to the under-evaluation agent. For positive control, Mitomycin C (Cayman Chemical, Ann Arbor, MI, USA) was used, a known clastogenic agent that induces micronuclei formation in dividing cells. The concentration used was 0.5  $\mu$ g/mL. Following treatment for 6 and 24 h, the medium was replaced with fresh medium containing Cytochalasin B (Cayman Chemical, Ann Arbor, MI, USA) (concentration used 3  $\mu$ g/mL) to inhibit cytokinesis, facilitating the formation of binucleated cells for scoring. Cells were incubated for an additional 19 h. Next, cells were fixed in ice-cold methanol for 15 min (HPLC and organic synthesis, high purity) (Charlotte, NC, USA). After air-drying, the cell nuclei and micronuclei were stained using Hoechst 33342 (5  $\mu$ g/mL) for 20 min at room temperature. Staining was performed in the dark to minimize photobleaching. Upon completion, cells were washed three times with PBS (Biosera, Cholet, France) to remove excess dye. Following a final air-drying step, the samples were analyzed using automated digital microscopy (Lionheart FX, Agilent BioTek, Winooski, VT, USA) at 4 $\times$  and 20 $\times$  magnification. Cells were evaluated by automated digital microscopy to determine the presence of cell lysis, cell detachment, cell viability, and observe possible morphological alterations.

Micronuclei were scored in a minimum of 1000 binucleated cells per condition, ensuring compliance with the scoring criteria outlined in ISO 10993-3, OECD, and ECVAM guidelines. Data interpretation involved determining the frequency of micronucleated cells and comparing treated groups to control groups (always in parallel with cytotoxicity assessments). Data preprocessing, processing, and analysis were carried out using

the BioTek Gen5 software v3.14 (BioTek Instruments, Winooski, VT, USA) for imaging and microscopy.

### 2.12. Hemolysis Assay

The assay was conducted according to the protocol from the American Society for Testing and Materials (ASTM) F756-17 [20] that is used by the FDA ([https://www.accessdata.fda.gov/scripts/cdrh/cfdocs/cfStandards/results.cfm?start\\_search=1&productcode=&category=&type=&title=&organization=3&referencenumber=&regulationnumber=&effectivedatefrom=&effectivedateto=&pagenum=500&sortcolumn=pad](https://www.accessdata.fda.gov/scripts/cdrh/cfdocs/cfStandards/results.cfm?start_search=1&productcode=&category=&type=&title=&organization=3&referencenumber=&regulationnumber=&effectivedatefrom=&effectivedateto=&pagenum=500&sortcolumn=pad); accessed on 10 October 2025). The assay was carried out using extract from the abovementioned materials that was obtained under the protocols ASTM F619-20 [21] and ISO 10993-Part 12 [17] “Sample preparation and reference materials”. Specifically, the extraction was carried out by incubating the material in phosphate-buffered saline (PBS), pH 7.3, for 3 days at 37 °C in borosilicate tubes (volume of buffer for plug electrode 2.435 mL; volume of buffer for cuff electrode 0.75 mL).

### 2.13. Complement Activation Assay

The sheep red blood cells (RBCs) in Alsever’s solution (Dunn Labortechnik GmbH) were washed multiple times in gelatin containing isotonic buffer. A small sample was withdrawn, lysed with pure water, and the concentration of cells·mL<sup>-1</sup> was determined by reading the absorbance of hemoglobin at 412 nm (absorbance of 0.56 corresponds to 1.5 × 10<sup>8</sup> sheep RBCs). Then, the optimal dilution of anti-sheep RBC antibody (R&D systems) was determined as described in the ASTM F1984-99 [19]. Initially, the antibody was reconstituted and incubated at 56 °C for 37 min to inactivate the potential endogenous complement component. The antibody was aliquoted and stored at -80 °C. The 1.5 × 10<sup>8</sup> RBCs were incubated with 1:2 serial dilutions of the antibody (1:400 to 1:25,600) at 37 °C for 10 min. Addition of human serum at 1:100 dilution was conducted followed by incubation at 37 °C for 1 h. During this incubation, lysis of RBC due to complement activation by the sensitized RBCs took place. After 1 h, the samples were centrifuged at 1000× g for 10 min at 4 °C and the absorbance of the supernatant was measured at 412 nm. The percentage of lysis was determined with the formula:

$$\% \text{ lysis} = \frac{\text{test absorbance} - \text{no RBC control absorbance}}{\text{total lysis absorbance}} \times 100$$

The optimal dilution was determined 1:400. Then, the plug and cuff electrodes were incubated with 300 µL human serum (Dunn Labortechnik GmbH), at 37 °C for 45 min. The serum was collected and diluted to 1:100 and tested for RBC lysis using 1:400 dilution of anti-sheep RBC antibody. As a control, lysis in the absence of antibody was used.

## 3. Results and Discussion

### 3.1. Biocompatibility of Plug and Cuff Electrode Against Neuronal Cells

The differentiated SH-SY5Y neuroblastoma cell line resembles the neuronal phenotype, and SH-SY5Y cells can easily differentiate to neuron-like cells upon exposure to 10 µM retinoic acid for 7 days [28]. Further, SH-SY5Y cells constitute a well-defined model of neuronal biocompatibility testing [29,30]. Initially, we tested the plug electrode for potential cytotoxicity. This experiment is important, since the primary application of the electrodes is in contact with the nerves. We performed two sequential extractions of the plug electrode, i.e., we obtained the first extract according to the ISO 10993-Part 12 and then, we re-extracted the electrode under the same conditions. Figure 2 shows the cytotoxicity results

for plug electrode against differentiated SH-SY5Y cells with the indirect method for the first extract, while Figure 3 shows the cytotoxicity for the second extract.

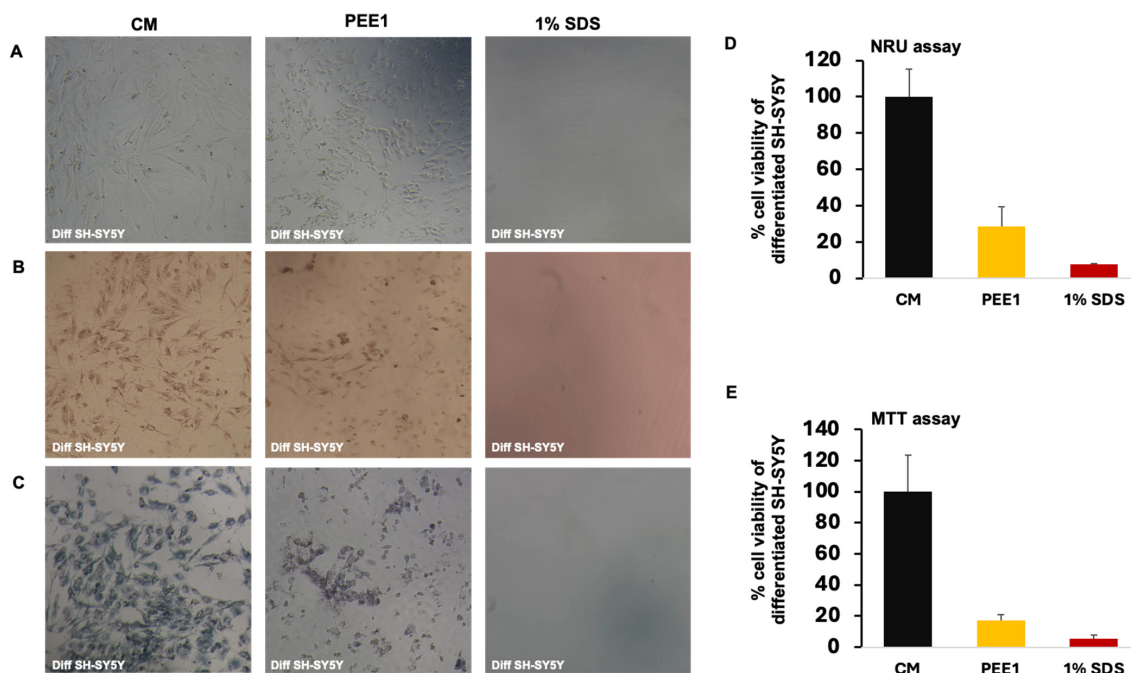


**Figure 2.** Assessment of in vitro cytotoxicity of first plug electrode extract (PEE1) on differentiated SH-SY5Y cells. (A), Representative photographs of differentiated SH-SY5Y treated with PEE for 24 h. (B), as A but stained with NRU. (C), as A but stained with MTT. (D), Quantification of cell viability measured with NRU. (E), Quantification of cell viability with MTT. Results are shown as median  $\pm$  SD of six replicates and three replicates for culture medium (CM), which is the negative control, and PEE, respectively. Sodium dodecyl sulfate (SDS) 1% was used as a positive control since it lyses the cells.

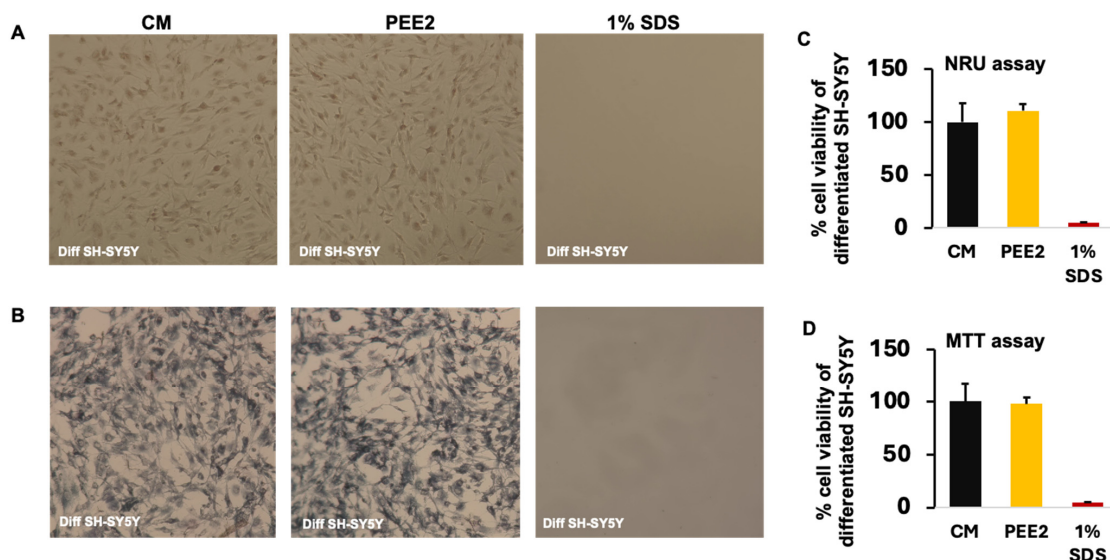


**Figure 3.** Assessment of in vitro cytotoxicity of second plug electrode extract (PEE2) on differentiated SH-SY5Y cells. (A), Representative photographs of differentiated SH-SY5Y treated with PEE for 24 h. (B), as A but stained with NRU. (C), as A but stained with MTT. (C), Quantification of cell viability measured with NRU. (D), Quantification of cell viability with MTT. Results are shown as median  $\pm$  SD of six replicates and three replicates for culture medium (CM), which is the negative control, and PEE, respectively. Sodium dodecyl sulfate (SDS) 1% was used as a positive control since it lyses the cells.

As can be deduced from Figures 2 and 3, the first extract shows significant cytotoxicity, which may indicate that residual chemicals from the production process remain in the device and need to be washed thoroughly before implantation. Accordingly, the second extract does not show any signs of cytotoxicity. Then, we moved to study the cuff electrode extract in an analogous way. Figure 4 shows the cytotoxicity of the first cuff electrode extract and Figure 5 shows the cytotoxicity of the second extract. No signs of cytotoxicity were observed either for the first or the second cuff electrode extract.

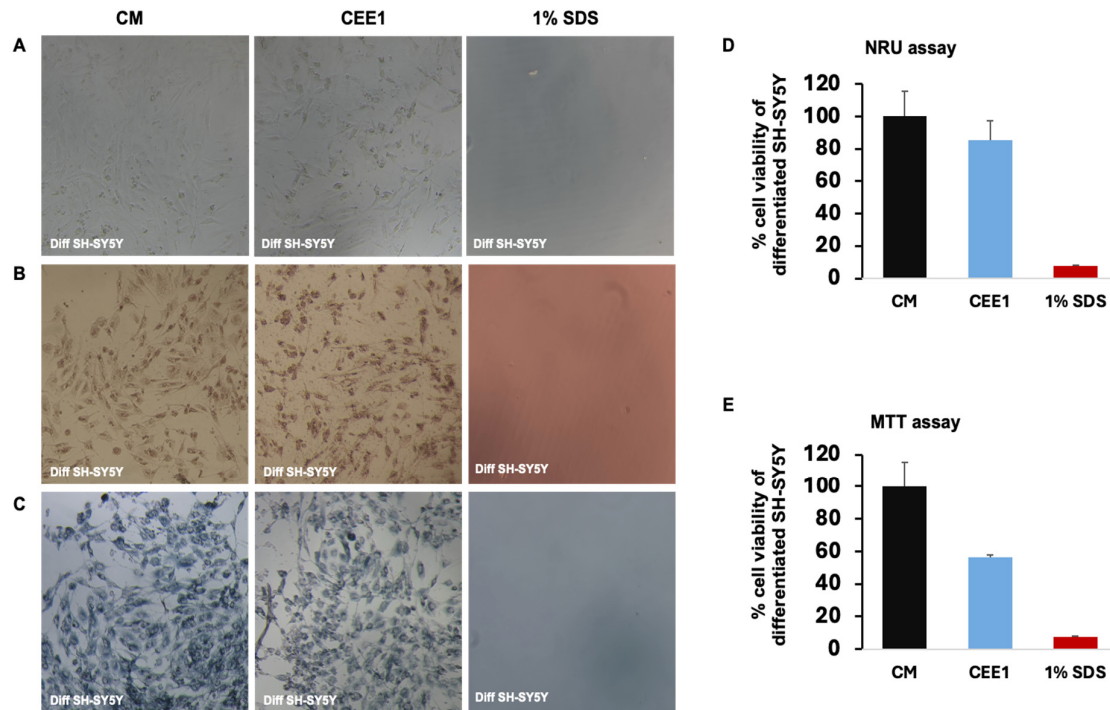


**Figure 4.** Assessment of in vitro cytotoxicity of first cuff electrode extract (CEE1) on differentiated SH-SY5Y cells. (A), Representative photographs of differentiated SH-SY5Y treated with CEE for 24 h. (B), as A but stained with NRU. (C), as A but stained with MTT. (D), Quantification of cell viability measured with NRU. (E), Quantification of cell viability with MTT. As positive control, 1% SDS was used.

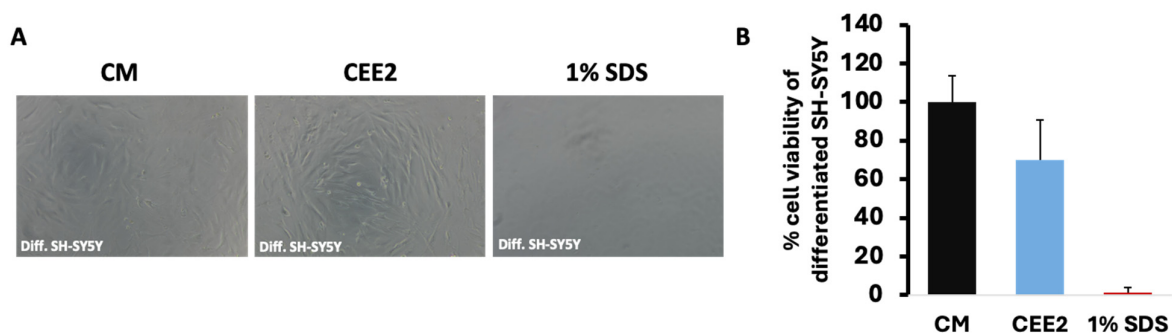


**Figure 5.** Assessment of in vitro cytotoxicity of second cuff electrode extract (CEE2) on differentiated SH-SY5Y cells. (A), Representative photographs of differentiated SH-SY5Y treated with CEE for 24 h. (B), Quantification of cell viability with MTT. As positive control, 1% SDS was used.

These results indicate that careful washing of electrodes should be carried out before they will be used in vivo. Probably residual solvents used during the preparation of electrodes contributed to the observed cytotoxicity of the first extract. Incubation of electrodes for 72 h in serum-free medium removes all toxic compounds, as only the first extract is

cytotoxic. Since the serum-free medium is a water-based medium, this indicates that an extended wash with ultrapure water before preclinical testing will suffice to remove all toxic residues.

At this point, the limitations of this assay should be outlined. Differentiated SH-SY5Y cells are neuronal-like cells and although they are extensively used for cytocompatibility testing they may provide data that differ from ones obtained from primary neuronal cells. An alternative approach could have involved the use of dorsal root ganglion cells (DRG), Schwann cells or a coculture of DRGs with Schwann cells [31,32]. DRGs are also applied to assess new tissue engineering models [32]. Schwann cells alone are primarily important in studies associated with regeneration, remyelination and neuroprotection. Nevertheless, in this study we applied the widely accepted SH-SY5Y model to overcome ethical issues associated with obtaining primary cells, which were not included in the NerveRepack project, and also to provide justification of the next step that is the preclinical assessment of the electrodes in pigs and sheep.

### 3.2. Biocompatibility of Plug and Cuff Electrode Against Fibroblasts

Both plug and cuff electrodes were tested for potential cytotoxicity against fibroblasts (NHDFs). The results for the plug electrode are shown in Figure 6 while the results for the cuff electrode in Figure 7. No signs of cytotoxicity were observed.

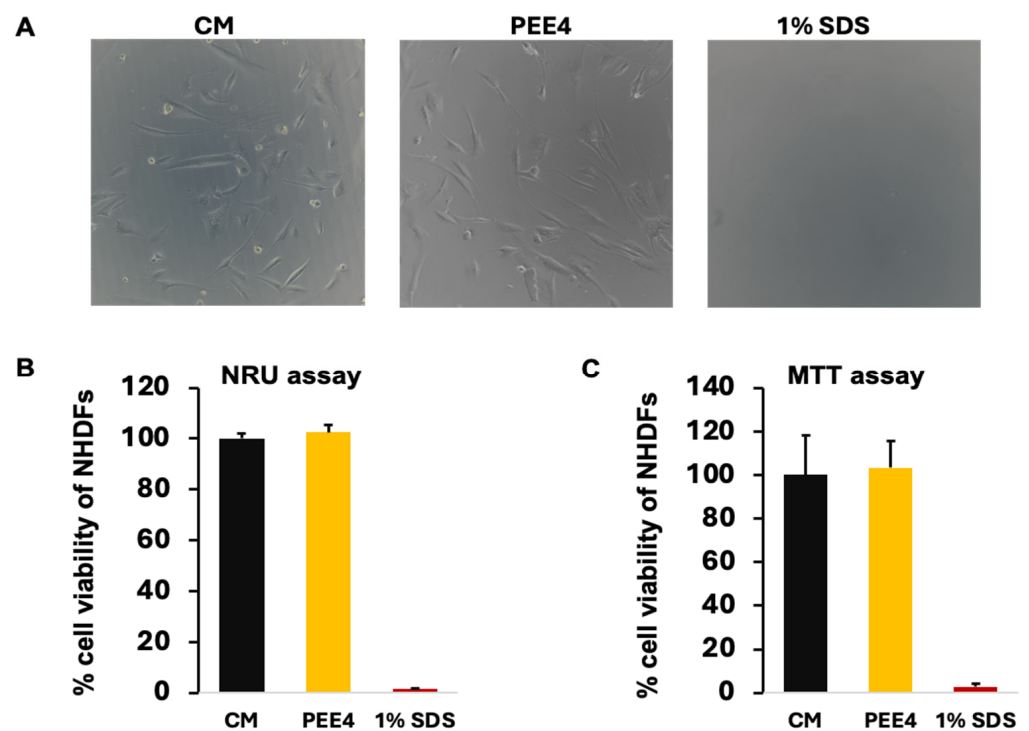


**Figure 6.** Assessment of in vitro cytotoxicity of plug electrode extract (PEE) on human fibroblasts. (A), Representative photographs of NHDFs treated with PEE for 24 h. (B), Quantification of cell viability measured with NRU. (C), Quantification of cell viability with MTT. As positive control, 1% SDS was used. Data are expressed as % viability of NHDFs in culture medium and are presented as median  $\pm$  SD. All reactions were performed in triplicate.

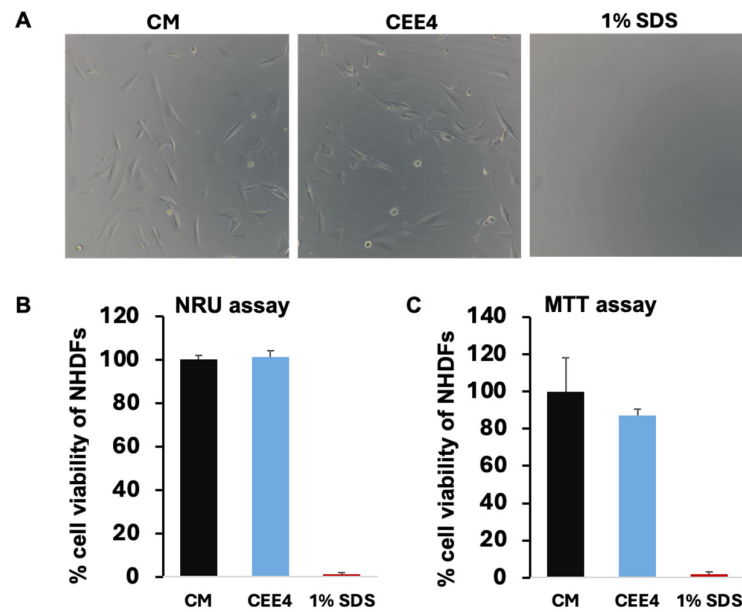


**Figure 7.** Assessment of in vitro cytotoxicity of cuff electrode extract (CEE) on human fibroblasts. (A), Representative photographs of NHDFs treated with CEE for 24 h. (B), Quantification of cell viability measured with NRU. (C), Quantification of cell viability with MTT. As positive control, 1% SDS was used. Data are expressed as % viability of NHDFs in culture medium and are presented as median  $\pm$  SD. All reactions were performed in triplicate.

### 3.3. Biocompatibility of Cuff Electrode Against Keratinocytes

Further, the cuff electrode extracts were tested for potential cytotoxicity against keratinocytes as described. The assessment of cytotoxicity was performed with Alamar Blue staining. As shown in Figure 8, no signs of cytotoxicity were found.

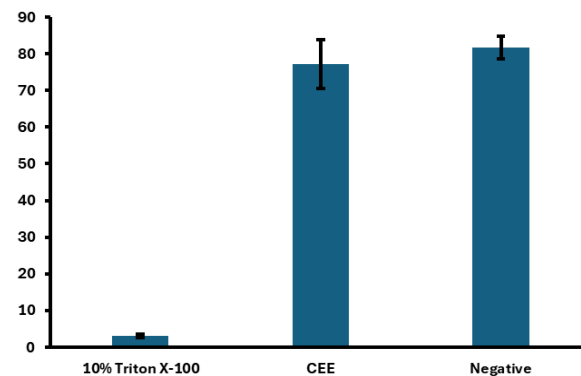


**Figure 8.** Assessment of in vitro cytotoxicity of cuff electrode extract (CEE) on HaCaT. 10% Triton-X 100 was used as positive control since it induces lysis of the cells.

### 3.4. Hemolytic Properties of Plug and Cuff Electrodes

Hemolysis assay is a classical assay used to test the hemocompatibility of the blood-contact artificial materials (biomaterials or implanted devices). Hemolysis results in the release of hemoglobin from red blood cells. Then, hemoglobin tetramer dissociates to dimers that translocate to various tissue barriers and exert toxic effects [33]. Therefore, for the therapeutic application of a new biomaterial or implant, it is a prerequisite that the tested material does not induce hemolysis. Indeed, as shown in Figure 9, both plug and cuff electrodes did not induce hemolysis.

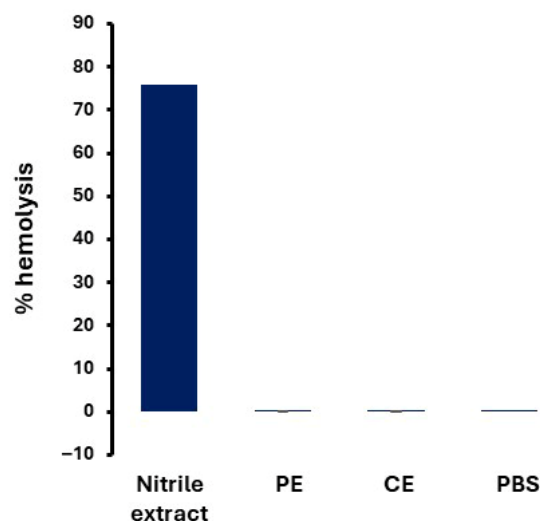


**Figure 9.** Assessment of hemolysis according to ASTM protocol F756-17. PE, plug electrode; CE, cuff electrode; Nitrile extract is the positive control and was produced by extraction of nitrile gloves with PBS at 121 °C for 30 min; PBS, is the negative control. PE and CE were tested in triplicates, while positive and negative controls were performed twice.

### 3.5. Complement Activation of Plug and Cuff Electrodes

The contact of an artificial material (implant or biomaterial) results in the adsorption of serum proteins on the surface of the material. Within the first minutes, the highly abundant proteins adsorb, like albumin, fibrinogen and IgGs. Afterwards, the less abundant proteins but with higher affinity for the surface displace the most abundant ones. In this direction, the C3 (and the IgGs) can bind to hydrophobic surfaces and activate the complement. This, in turn, can lead to the development of an inflammatory reaction. Therefore, testing for activation of complement by a biomaterial or implant is an important assay that should be carried out during the evaluation process of an artificial material. The assay was carried out with the ASTM F1984-99 protocol, which is based on the fact that complement activation factors are depleted from the serum when it is incubated with the tested material. Then the “depleted” serum is tested for its ability to induce complement activation and lysis of RBCs. Thus, if a material does not activate the complement, it will yield high levels of RBC lysis. As shown in Figure 10, the cuff electrode does not activate the complement. In contrast, the plug electrode shows significant signs of complement activation, at levels comparable to cellulose (used as a positive control). It should be noted that this assay is a prediction for the potential complement activation in vivo. Therefore, the plug electrode that shows the ability to activate the complement in the ASTM F1984-99 does not necessarily mean that it will activate the complement in vivo, and in vivo studies should be carried out and carefully evaluated. There are cases where material can activate complement in vitro but not in vivo. For example, adenoviral virions activate complement in vitro but in vivo a completely different mechanism operates. Specifically, in vitro virions activate the complement through an antibody-mediated process, while in vivo the entry-deficient adenoviral virions are unable to activate the complement [34]. Further, testing of individual components of the plug electrode may provide a clue on which component causes the complement activation and whether this can be changed with an alternative one. Finally, the fact that a potential activation of complement may not preclude its clinical application comes from the observation that almost all orthopedic biomaterials activate the complement system [35].

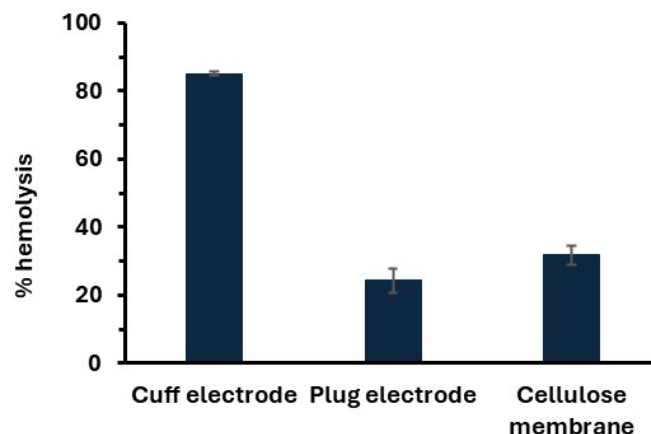


**Figure 10.** Complement activation by plug and cuff electrode. The assay is based on complement depletion upon incubation of the serum with the tested material; thus, the lower the level of RBC lysis, the higher the ability to induce complement activation. Cellulose membrane was used as a control that induces complement activation.

### 3.6. Genotoxicity/Carcinogenicity Evaluation of Plug and Cuff Electrodes

Genotoxicity/carcinogenicity assessment was performed at two timepoints, 6 and 24 h, modeling short- and long-term exposure, respectively. Initially, the cytotoxicity of CHO cells against the plug and the cuff electrode in question was determined. The choice of CHO cells in genotoxicity/carcinogenicity assays is well documented in the literature [36], well-established in industry, and importantly, it is recommended by the Organization for the Economic Co-operation and Development (OECD)—Test 479 ([https://www.oecd.org/en/publications/test-no-479-genetic-toxicology-in-vitro-sister-chromatid-exchange-assay-in-mammalian-cells\\_9789264071384-en.html](https://www.oecd.org/en/publications/test-no-479-genetic-toxicology-in-vitro-sister-chromatid-exchange-assay-in-mammalian-cells_9789264071384-en.html); accessed on 10 October 2025), the ISO 10993-3, and the ASTM E1262 [18]. Since CHO cells are of mammalian origin, they provide a relevant model, indicative of potential genotoxicity/carcinogenicity effects in human cells.

The genotoxicity/carcinogenicity and the cytotoxicity results of the plug electrode extract are presented in Table 3. No significant alterations were detected in either cellular metabolic activity or viability following the exposure of the CHO cells to the plug electrode extract for 6 or 24 h. Conversely, a significant reduction in both parameters was observed at 24 h in cells treated with the positive control (mitomycin-C).

**Table 3.** Cytotoxicity and micronuclei frequency of CHO cells, under short and long exposure to the plug electrode extract (PEE).

Test Conditions	Cell Viability (%)		Micronuclei Frequency (%)	
	6 h	24 h	6 h	24 h
CytoB + AB			9	10
MMC + CytoB + AB	100	77	10	29
Control extract + CytoB + AB	95	84	9	12
PEE + CytoB + AB	100	100	9	18

\* The assay was carried out in triplicate. \*\* For cytotoxicity, normalization of all testing conditions was performed against CytoB + AB: Cytochalasin-B in the presence of the Alamar Blue dye. \*\*\* MMC + CytoB + AB: Mitomycin-C in the presence of cytochalasin-B and the Alamar Blue dye. \*\*\*\* Control extract + CytoB + AB: CHO cell culture supernatant in the absence of the plug electrode extract (72 h exposure, “Extract—Indirect Biocompatibility Test”), in the presence of cytochalasin-B and the Alamar Blue dye. \*\*\*\*\* PEE + CytoB + AB: CHO cell culture supernatant in the presence of the plug electrode, Plug electrode (72 h exposure, “Extract—Indirect Biocompatibility Test”), in the presence of cytochalasin-B and the Alamar Blue dye.

Metabolic activity measurements using the Alamar Blue assay further supported the in vitro biocompatibility of the plug electrode. Cells exposed to the plug electrode extract

demonstrated metabolic activity levels comparable to the control group, confirming the material's non-toxic profile.

To evaluate the genotoxic and/or carcinogenic potential of the plug electrode, the micronucleus assay was performed, and the Micronuclei Frequency (%) was calculated, as shown in Table 3. This parameter is defined as the percentage of binucleated cells containing micronuclei and serves as a key indicator of genotoxicity and is calculated by the following formula: Micronucleus Frequency (MN) = (Number of binucleated cells with micronuclei/Total number of binucleated cells analyzed)  $\times$  100.

The results revealed no statistically significant increase in micronucleus frequency in samples treated with the plug electrode extract compared to control conditions. These findings suggest that the plug electrode does not induce chromosomal damage or genomic instability.

Consistent with these results, no observable alterations were noted in cell morphology, detachment, or lysis. Representative images for both time points (6 and 24 h) are shown in Figure 11.

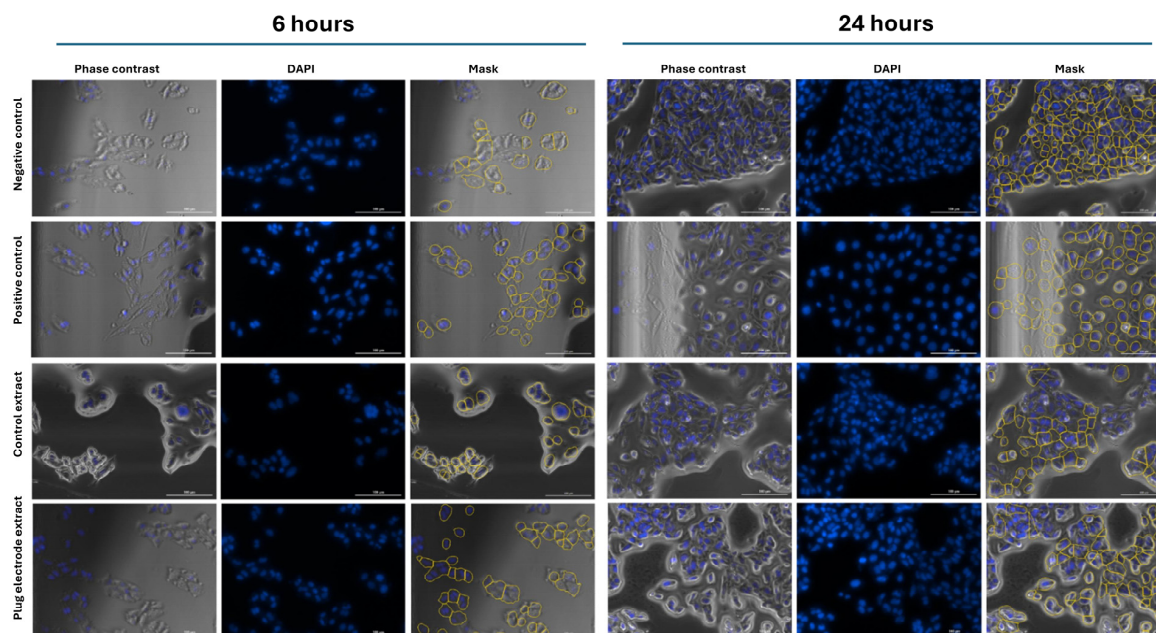


**Figure 11.** Micronucleus assay outcomes for the plug electrode at 6 h (short-term exposure) and 24 h (long-term exposure). CHO cells were visualized by automated digital microscopy (Agilent BioTek Lionheart FX; Santa Clara, CA, USA). Phase contrast provides morphological information and enables qualitative assessment as per ISO 10993. DAPI staining allows for nuclei staining. Image processing was carried out using BioTek Gen 5 v3.14 software along with automated detection of the regions of interest (ROIs). Negative control = CHO cells in complete culture medium; Positive control = CHO cells in the presence of Mitomycin C; Control extract = CHO cells in the absence of the plug electrode extract (72 h exposure, “Extract—Indirect Biocompatibility Test”); Plug electrode extract = CHO cells in the presence of the plug electrode extract (72 h exposure, “Extract—Indirect Biocompatibility Test”). Each image included in this panel corresponds to a scale bar of 100  $\mu$ m.

Proceeding with the cytotoxicity based on Alamar Blue, for the cuff electrode the results are presented in Table 4. Findings support the notion that the exposure to mitomycin C (positive control) led to a notable decrease in both metabolic function and cell viability after 24 h of exposure, as anticipated given its known genotoxic properties. According to Table 4, the cells exposed to the cuff electrode extract exhibited metabolic activity comparable to that of the control group, confirming the non-toxic nature of the material. Furthermore, no changes in cell morphology, detachment, and/or lysis were observed.

**Table 4.** Cytotoxicity and micronuclei frequency of CHO cells, under short and long exposure to the cuff electrode extract (CEE).

Test Conditions	Cell Viability (%)		Micronuclei Frequency (%)	
	6 h	24 h	6 h	24 h
CytoB + AB			9	11
MMC + CytoB + AB	88	52	23	22
Control extract + CytoB + AB	100	99	10	12
CEE + CytoB + AB	100	75	12	15

\* The assay was carried out in triplicate. Results are presented as mean  $\pm$  SD. \*\* For cytotoxicity, normalization of all testing conditions was performed against CytoB + AB: Cytochalasin-B in the presence of the Alamar Blue dye. \*\*\* MMC + CytoB + AB: Mitomycin-C in the presence of cytochalasin-B and the Alamar Blue dye. \*\*\*\* Control extract + CytoB + AB: CHO cell culture supernatant in the absence of the cuff electrode extract (72 h exposure, “Extract—Indirect Biocompatibility Test”), in the presence of cytochalasin-B and the Alamar Blue dye. \*\*\*\*\* CEE + CytoB + AB: CHO cell culture supernatant in the presence of the cuff electrode, Cuff electrode (72 h exposure, “Extract—Indirect Biocompatibility Test”), in the presence of cytochalasin-B and the Alamar Blue dye.

The results presented in Table 4 reveal no statistically significant increase in micronuclei frequency (%) in cells treated with the cuff electrode extract compared to control conditions, supporting the biocompatibility of this material. Moreover, an increase in micronuclei frequency (%) was observed in the presence of the positive control (mitomycin-C), confirming the reliability of the method. Taking into consideration the above, no two-fold increase in micronuclei was detected in any electrode-exposed group.

The digital microscopy pictures for short-term (6 h) and long-term (24 h) exposures are shown in Figure 12.

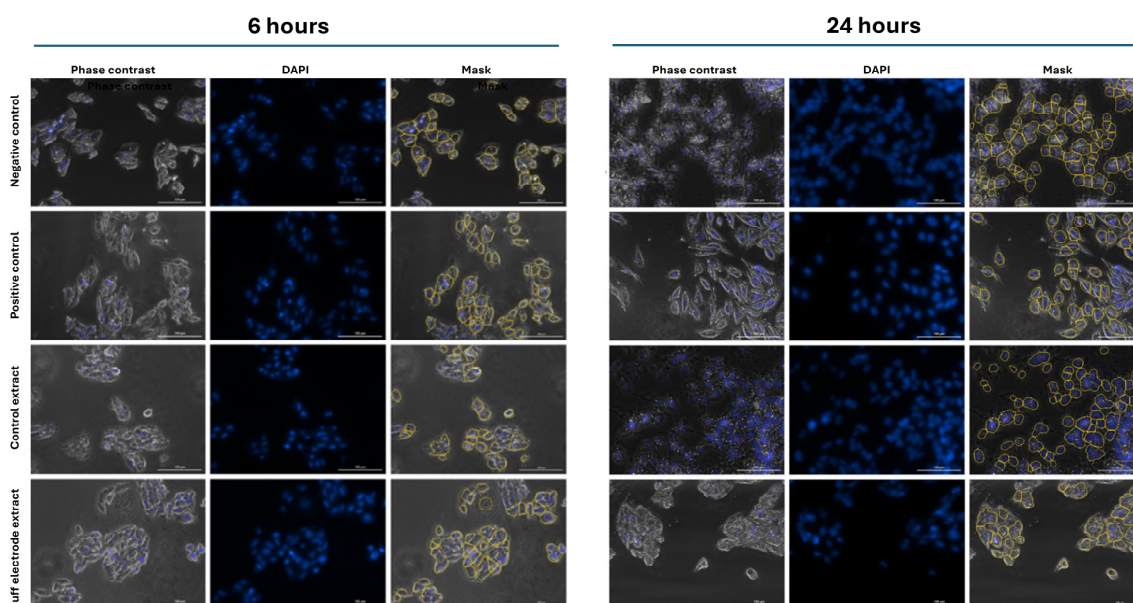


**Figure 12.** Micronucleus assay outcomes for the cuff electrode at 6 h (short-term exposure) and 24 h (long-term exposure). CHO cells were visualized by automated digital microscopy (Agilent BioTek Lionheart FX). Phase contrast provided morphological information and enabled qualitative assessment as per ISO 10993. DAPI staining allows for nuclei staining. Image processing was carried out using BioTek Gen 5 v3.14 software along with automated detection of the regions of interest (ROIs). Negative control = CHO cells in complete culture medium; Positive control = CHO cells in the presence of Mitomycin C; Control extract = CHO cells in the absence of the cuff electrode extract (72 h exposure, “Extract—Indirect Biocompatibility Test”); Cuff electrode extract = CHO cells in the presence of the cuff electrode extract (72 h exposure, “Extract—Indirect Biocompatibility Test”). Each image included in this panel corresponds to a scale bar of 100  $\mu$ m.

#### 4. Limitations of the Study

The study has certain limitations that need to be pointed out. The main limitation deals with the use of an indirect assay which mainly detects the effects caused by chemicals leaching from biomedical devices. However, this assay cannot address the potential effect of the surface, as it is known that certain characteristics of the surface (e.g., the contact angle) may have serious effects on the attachment or growth of cells [37]. Due to the restricted number of plug and cuff electrode prototypes that were fabricated, it was decided to proceed as described herein.

Another issue that has not been investigated is the potential adsorption of protein on the surface of the electrodes which may affect the bidirectional communication and electrochemical performance. This can be easily addressed after implanting the electrodes in preclinical models for a certain period, e.g., 30 days, followed by removal of the electrodes and analysis by Raman microspectroscopy as performed previously [37].

Another factor that was not addressed here is the potential induction of macrophage activation and perineural fibrosis. In a previous small scale preclinical assessment of the plug electrode implanted in two pigs, no signs of fibrosis or inflammation were detected after 10 days [38]. Finally, the cuff electrode has been designed to be flexible to reduce the potential of inducing fibrosis, and this will be investigated in future in vivo studies.

Despite the limitations presented, all experiments were conducted in accordance with ISO, ECVAM, OECD, and ASTM standards as depicted in Table 5.

**Table 5.** Synopsis of the guidelines followed in this study.

Test or Procedure	ISO	ASTM	Comment
Extract preparation	ISO 10993-2 [14]	ASTM F619-20	Similar procedures between ISO and ASTM
Cytotoxicity Testing	ISO 10993		
Hemocompatibility Testing	ISO 10993-1 [39], ISO 10993-4 [40]	ASTM F756-17 (hemolysis) ASTM F1984-99 (complement activation)	Used by the FDA
Genotoxicity/ Carcinogenicity Testing	ISO 10993-3		OECD ECVAM

#### 5. Conclusions

NerveRepack is a European research project focused on advancing neuroprosthetic technologies through the development of interfaces between injured peripheral nerves and external biomimetic devices, such as exoskeletons and exoprostheses, for amputated or paralyzed individuals. The project aims to support improved interaction between neural signals and assistive devices, with the broader goal of enhancing functional outcomes and quality of life.

A central objective of NerveRepack is the development of implantable neural interfaces capable of safely transmitting neural signals to external devices and receiving sensory feedback from integrated sensors. Within this framework, plug and cuff electrodes have been designed to enable communication between the patient's nervous system and sensor-equipped exoskeletons or exoprostheses. Consequently, the safety and biocompatibility of these electrodes represent key design considerations.

The biocompatibility of the selected implant technologies used in the fabrication of the plug and cuff electrodes was evaluated using in vitro assays conducted in accordance with relevant ISO, ECVAM, OECD, and ASTM standards, as summarized in Table 5. The results

did not reveal cytotoxic effects across the tested cell types, nor evidence of genotoxicity or mutagenicity under the applied experimental conditions.

Thus, our tests confirm that the selected technologies, materials and processes are suitable for long-term implants. With completed testing and validations for active implantable medical devices, they will be ready for the in vivo implantation, to determine their performance.

**Author Contributions:** Conceptualization, E.Z., A.K., G.P., G.S. (Georgia Sotiropoulou), T.K., C.M., M.I., O.N.I., D.D., E.F., G.S. (Gerd Siekmeyer) and P.G.; methodology, E.Z., A.K., G.P., G.S. (Georgia Sotiropoulou), N.R., A.S., L.G., T.K., P.Ś., L.M.-K. and K.G.-J.; software, N.R., A.S., L.G. and T.K.; validation, E.Z., A.K., G.P., G.S. (Georgia Sotiropoulou), N.R., A.S., L.G., T.K., P.Ś., L.M.-K. and K.G.-J.; formal analysis, E.Z., A.K., G.P., G.S. (Georgia Sotiropoulou), N.R., A.S., L.G. and T.K.; investigation, E.Z., A.K., G.P., G.S. (Georgia Sotiropoulou), N.R., A.S., L.G., T.K., P.Ś., L.M.-K. and K.G.-J.; resources, G.S. (Georgia Sotiropoulou), T.K. and K.G.-J.; data curation, N.R., A.S., L.G. and T.K.; writing—original draft preparation, E.Z., G.P., N.R., A.S., L.G. and K.G.-J.; writing—review and editing, C.M., M.I., T.K., G.S. (Georgia Sotiropoulou), G.P., E.Z. and K.G.-J.; visualization, N.R., A.S., L.G. and T.K.; supervision, G.P., G.S. (Georgia Sotiropoulou), T.K. and K.G.-J.; project administration, G.S. (Georgia Sotiropoulou), N.R., T.K. and K.G.-J.; funding acquisition, G.S. (Georgia Sotiropoulou), T.K. and K.G.-J. All authors have read and agreed to the published version of the manuscript.

**Funding:** This paper is co-funded by the European Union’s Horizon Europe research and innovation programme under grant agreement No. 101112347, project NerveRepack (Intelligent neural system for bidirectional connection with exoprostheses and exoskeletons) and supported by the CHIPS Joint Undertaking and its members.

**Institutional Review Board Statement:** Not applicable.

**Informed Consent Statement:** Not applicable.

**Data Availability Statement:** All data are included in the manuscript.

**Conflicts of Interest:** Authors Gerd Siekmeyer and Patrick Grottemeyer were employed by the company Acquandas. The remaining authors declare that the research was conducted in the absence of any commercial or financial relationships that could be construed as a potential conflict of interest.

## Abbreviations

The following abbreviations are used in this manuscript:

ASTM	American Society for Testing and Materials
CEE	Cuff electrode extract
ISO	International Organization for Standardization
MTT	3-(4,5-dimethylthiazol-2-yl)-2,5-diphenyltetrazolium-bromide)
NR	Neutral Red
PEE	Plug electrode extract

## References

1. Lv, S.; Xu, Z.; Mo, F.; Wang, Y.; Duan, Y.; Liu, Y.; Jing, L.; Shan, J.; Jia, Q.; Wang, M.; et al. Long-term stability strategies of deep brain flexible neural interface. *npj Flex. Electron.* **2025**, *9*, 40. [[CrossRef](#)]
2. Russell, C.; Roche, A.D.; Chakrabarty, S. Peripheral nerve bionic interface: A review of electrodes. *Int. J. Intell. Robot. Appl.* **2019**, *3*, 11–18. [[CrossRef](#)]
3. Feng, C.; Frewin, C.L.; Tanjil, M.R.E.; Everly, R.; Bieber, J.; Kumar, A.; Wang, M.C.; Sadow, S.E. A flexible a-sic-based neural interface utilizing pyrolyzed-photoresist film (C) active sites. *Micromachines* **2021**, *12*, 821. [[CrossRef](#)] [[PubMed](#)]
4. Yildiz, K.A.; Shin, A.Y.; Kaufman, K.R. Interfaces with the peripheral nervous system for the control of a neuroprosthetic limb: A review. *J. Neuroeng. Rehabil.* **2020**, *17*, 43. [[CrossRef](#)]
5. Wu, J.; Han, Q.; Gui, D.; Qian, Y. Multidimensional advances in neural interface technology for peripheral nerve repair: From material innovation to clinical translation. *Mater. Today Bio* **2025**, *34*, 102092. [[CrossRef](#)]

6. Delianides, C.; Tyler, D.; Pinault, G.; Ansari, R.; Triolo, R. Implanted high density cuff electrodes functionally activate human tibial and peroneal motor units without chronic detriment to peripheral nerve health. *Neuromodulation* **2020**, *23*, 754–762. [[CrossRef](#)]
7. Luan, L.; Robinson, J.T.; Aazhang, B.; Chi, T.; Yang, K.; Li, X.; Rathore, H.; Singer, A.; Yellapantula, S.; Fan, Y.; et al. Recent advances in electrical neural interface engineering: Minimal invasiveness, longevity, and scalability. *Neuron* **2020**, *108*, 302–321. [[CrossRef](#)]
8. Ranke, D.; Lee, I.; Gershanok, S.A.; Jo, S.; Trotto, E.; Wang, Y.; Balakrishnan, G.; Cohen-Karni, T. Multifunctional nanomaterials for advancing neural interfaces: Recording, stimulation, and beyond. *Acc. Chem. Res.* **2024**, *57*, 1803–1814. [[CrossRef](#)]
9. Liu, Z.Q.; Yu, X.Y.; Huang, J.; Wu, X.Y.; Wang, Z.Y.; Zhu, B.P. A review: Flexible devices for nerve stimulation. *Soft Sci.* **2024**, *4*, 4. [[CrossRef](#)]
10. Debnath, S.; Prins, N.W.; Pohlmeier, E.; Mylavarapu, R.; Geng, S.; Sanchez, J.C.; Prasad, A. Long-term stability of neural signals from microwire arrays implanted in common marmoset motor cortex and striatum. *Biomed. Phys. Eng. Express* **2018**, *4*, 055025. [[CrossRef](#)]
11. Rokaya, D.; Skallevoid, H.E.; Srimaneepong, V.; Marya, A.; Shah, P.K.; Khurshid, Z.; Zafar, M.S.; Sapkota, J. Shape Memory Polymeric Materials for Biomedical Applications: An Update. *J. Compos. Sci.* **2023**, *7*, 24. [[CrossRef](#)]
12. Choi, Y.S.; Hsueh, Y.Y.; Koo, J.; Yang, Q.; Avila, R.; Hu, B.; Xie, Z.; Lee, G.; Ning, Z.; Liu, C.; et al. Stretchable, dynamic covalent polymers for soft, long-lived bioresorbable electronic stimulators designed to facilitate neuromuscular regeneration. *Nat. Commun.* **2020**, *11*, 5990. [[CrossRef](#)] [[PubMed](#)]
13. Chapman, C.A.R.; Chen, H.; Stamou, M.; Biener, J.; Biener, M.M.; Lein, P.J.; Seker, E. Nanoporous gold as a neural interface coating: Effects of topography, surface chemistry, and feature size. *ACS Appl. Mater. Interfaces* **2015**, *7*, 7093–7100. [[CrossRef](#)] [[PubMed](#)]
14. ISO 10993; Biological Evaluation of Medical Devices. Part 2 “Animal Welfare Requirements” 3rd Edition. International Organization for Standardization (ISO): Geneva, Switzerland, 2022.
15. ISO 10993; Biological Evaluation of Medical Devices. Part 3 “Tests for Genotoxicity, Carcinogenicity, and Reproductive Toxicity” 3rd Edition. International Organization for Standardization (ISO): Geneva, Switzerland, 2014.
16. ISO 10993; Biological Evaluation of Medical Devices. Part 5 “Tests for In Vitro Cytotoxicity” 3rd Edition. International Organization for Standardization (ISO): Geneva, Switzerland, 2009.
17. ISO 10993; Biological Evaluation of Medical Devices. Part 12 “Sample Preparation and Reference Materials” 5th Edition. International Organization for Standardization (ISO): Geneva, Switzerland, 2021.
18. ASTM E1262-88; Standard Guide for Performance of Chinese Hamster Ovary Cell/Hypoxanthine Guanine Phosphoribosyl Transferase Gene Mutation Assay. ASTM International: West Conshohocken, PA, USA, 2018.
19. ASTM F1984-99; Standard Practice for Testing for Whole Complement Activation in Serum by Solid Materials. ASTM International: West Conshohocken, PA, USA, 2018.
20. ASTM F756-17; Standard Practice for Assessment of Hemolytic Properties of Materials. ASTM International: West Conshohocken, PA, USA, 2017.
21. ASTM F619-20; Standard Practice for Extraction of Materials Used in Medical Devices. ASTM International: West Conshohocken, PA, USA, 2025.
22. Melvin, T. The European Medical Device Regulation-What Biomedical Engineers Need to Know. *IEEE J. Transl. Eng. Health Med.* **2022**, *10*, 4800105. [[CrossRef](#)] [[PubMed](#)]
23. Rêgo, S.; Dutra-Medeiros, M.; Nunes, F. The Challenges of Setting Up a Clinical Study with the New European Union Medical Device Regulation. *Acta Med. Port.* **2023**, *36*, 455–457. [[CrossRef](#)]
24. Boyle, G.; Melvin, T.; Verdaasdonk, R.M.; Van Boxtel, R.A.; Reilly, R.B. Hospitals as medical device manufacturers: Keeping to the Medical Device Regulation (MDR) in the EU. *BMJ Innov.* **2024**, *10*, 74–80. [[CrossRef](#)]
25. Lienemann, S.; Donahue, M.J.; Zötterman, J.; Farnebo, S.; Tybrandt, K. A soft and stretchable multielectrode cuff for selective peripheral nerve stimulation. *Adv. Mater. Technol.* **2023**, *8*, 2201322. [[CrossRef](#)]
26. Róžańska, A.; Walkowicz, M.; Bulanda, M.; Kasperski, T.; Synowiec, E.; Osuch, P.; Chmielarczyk, A. Evaluation of the efficacy of UV-C radiation in eliminating microorganisms of special epidemiological importance from touch surfaces under laboratory conditions and in the hospital environment. *Healthcare* **2023**, *11*, 3096. [[CrossRef](#)]
27. Rampersand, S.N. Multiple application of Alamar blue as an indicator of metabolic function and cellular health in cell viability bioassays. *Sensors* **2012**, *12*, 12347–12360. [[CrossRef](#)]
28. Kovalevich, J.; Langford, D. Considerations for the use of SH-SY5Y neuroblastoma cells in neurobiology. *Methods Mol. Biol.* **2013**, *1078*, 9–21.
29. Yoon, S.B.; Lee, G.; Park, S.B.; Cho, H.; Lee, J.O.; Koh, B. Properties of differentiated SH-SY5Y grown on carbon-based materials. *RSC Adv.* **2020**, *10*, 19382. [[CrossRef](#)]

30. Buttiglione, M.; Vitiello, F.; Sardella, E.; Petrone, L.; Nardulli, M.; Favia, P.; d'Agostino, R.; Gristino, R. Behaviour of SH-SY5Y neuroblastoma cell line grown in different media and on different chemically modified substrates. *Biomaterials* **2007**, *28*, 2932–2945. [[CrossRef](#)] [[PubMed](#)]
31. Pawelec, K.M.; Hix, J.M.L.; Shapiro, E.M. Material matters: Degradation products affect regenerating Schwann cells. *Biomater. Adv.* **2024**, *159*, 213825. [[CrossRef](#)] [[PubMed](#)]
32. Zou, Z.; Zheng, Q.; Wu, Y.; Guo, X.; Yang, S.; Li, J.; Pan, H. Biocompatibility and bioactivity of designer self-assembling nanofiber scaffold containing FGL motif for rat dorsal root ganglion neurons. *J. Biomed. Mater. Res. A* **2010**, *95*, 1125–1131. [[CrossRef](#)] [[PubMed](#)]
33. Tian, J.; Xu, Z.; Smith, J.S.; Hofherr, S.E.; Barry, M.A.; Byrnes, A.P. Adenovirus activates complement by distinctly different mechanisms in vitro and in vivo: Indirect complement activation by virions in vivo. *J. Virol.* **2009**, *83*, 5648–5658. [[CrossRef](#)]
34. Mödinger, Y.; Teixeira, G.Q.; Neidlinger-Wilke, C.; Ignatius, A. Role of the complement system in the response to orthopedic biomaterials. *Int. J. Mol. Sci.* **2018**, *19*, 3367. [[CrossRef](#)]
35. Vallelian, F.; Buehler, P.W.; Schaer, D.J. Hemolysis, free hemoglobin toxicity, and scavenger protein therapeutics. *Blood* **2022**, *140*, 1837–1844. [[CrossRef](#)]
36. Erexson, G.L.; Periago, M.V.; Spicer, C.S. Differential sensitivity of Chinese hamster V79 and Chinese hamster ovary (CHO) cells in the in vitro micronucleus screening assay. *Mutation Res.* **2001**, *495*, 75–80. [[CrossRef](#)]
37. Zingkou, E.; Kolianou, A.; Angelis, G.; Lykouras, M.; Orkoula, M.; Pampalakis, G.; Sotiropoulou, G. Cytocompatibility study of stainless steel 316l against differentiated SH-SY5Y cells. *Biomimetics* **2025**, *10*, 169. [[CrossRef](#)]
38. Ionescu, O.N.; Franti, E.; Carbutaru, V.; Moldovan, C.; Dinulescu, S.; Ion, M.; Dragomir, D.C.; Mihailescu, C.M.; Lascar, I.; Oproiu, A.M.; et al. System of implantable electrodes for neural signal acquisition and stimulation for wirelessly connected forearm prosthesis. *Biosensors* **2024**, *14*, 31. [[CrossRef](#)]
39. ISO 10993; Biological Evaluation of Medical Devices. Part 1 “Requirements and General Principles for the Evaluation of Biological Safety Within a Risk Management Process” 5th Edition. International Organization for Standardization (ISO): Geneva, Switzerland, 2025.
40. ISO 10993; Biological Evaluation of Medical Devices. Part 4 “Selection of Tests for Interactions with Blood” 3rd Edition. International Organization for Standardization (ISO): Geneva, Switzerland, 2017.

**Disclaimer/Publisher’s Note:** The statements, opinions and data contained in all publications are solely those of the individual author(s) and contributor(s) and not of MDPI and/or the editor(s). MDPI and/or the editor(s) disclaim responsibility for any injury to people or property resulting from any ideas, methods, instructions or products referred to in the content.